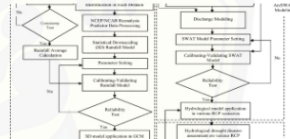## Natural Hazards

Volume 112, issue 2, June 2022

34 articles in this issue

Assessment of climate change impact on drought disaster in Sampean Baru watershed, East Java, Indonesia based on IPCC-AR5

Gusfan Halik, Victorius Setiaji Putra & Retno Utami Agung Wiyono

Original Paper | Published: 18 February 2022

Pages: 1705 - 1726

https://link.springer.com/article/10.1007/s11069-022-05245-7

Natural Hazards

Q1
Earth and Planetary Sciences (miscellaneous)
best quartile

SJR 2021
0.7

powered by scimagojr.com

https://www.scimagojr.com/journalsearch.php?q=23282&tip=sid&clean=0

ORIGINAL PAPER

Assessment of climate change impact on drought disaster in Sampean Baru watershed, East Java, Indonesia based on IPCC-AR5

Gusfan Halik[1] · Victorius Setiaji Putra[1] · Retno Utami Agung Wiyono[1]

Abstract

This research had been conducted in Sampean Baru Watershed, Bondowoso-Situbondo Regency, Indonesia. The National Disaster Management Agency (BNPB) categorizes this watershed as an area that has a very high level of drought. This condition is likely to get worse and will have a broad impact on people's lives if global warming continues for the next few years, therefore, future drought assessment is needed to assist in decision making. This study aims to assess future drought using General Circulation Model data. The GCM data contains future climate change scenarios called the Representatives Concentration Pathway (RCP) as results of the Fifth Assessment Report-Intergovernmental Panel on Climate Change (IPCC-AR5) report. GCM data containing coarse-resolution climate parameters are processed using downscaling techniques, so predictive rainfall data with the fine resolution, and local scale are obtained. The rainfall data is used in Soil and Water Assessment Tools (SWAT) modelling to simulate discharge at Sampean Baru watershed. Furthermore, the Standardized Runoff Index (SRI) method with simulated discharge used as input data to assess the drought severity. The results showed that the drought severity using SRI gives high accuracy and can be used for predictions of drought in the future. The drought prediction results showed that increased greenhouse gas concentrations while earth's temperature on RCP scenarios have an influence the intensity of drought events and drought-affected areas. Scenarios of climate change based on the temperature increase contained in the RCP will have a real effect on the severity of drought.

Keywords Drought assessment · SWAT model · GCM · RCP scenarios · SRI

Abbreviations
ANN   Artificial Neural Networks
BIG   Geospatial Information Agency
BNPB   The National Disaster Management Agency
BPBD   The Regional Disaster Management Agency
DD   Dynamic Downscaling

✉ Gusfan Halik
   gusfan.teknik@unej.ac.id

1   Civil Engineering Department, Engineering Faculty, University of Jember, P.O. Box 159, Jember, East Java, Indonesia

DEM	Digital Elevation Model
GHG	Greenhouse gases
IPCC	The Intergovernmental Panel on Climate Change
PDAM	The Regional Water Supply Company
RCP	The Representative Concentration Pathway
SD	Statistical Downscaling
SPI	Standardized Precipitation Index
SRES	The Special Report on Emission Scenarios
SRI	Standardized Runoff Index
USGS	The United States Geological Survey

1 Introduction

Climate change should be the main concern of every human being on earth. Today, human sensitivity in maintaining the condition of the earth has diminished. Greenhouse gases (GHG) resulting from human activities (anthropogenic) are getting more and more numerous (Anderson et al. 2016). It changes the composition of the GHG that make up the atmosphere so that in the process, sunlight that should be reflected outside the earth through the atmosphere becomes trapped on the earth (Kweku et al. 2018). Sunlight trapped on the earth increases the earth's temperature from its normal conditions so that the earth becomes warmer (global warming) (Sudarma and As-syakur 2018). Also, global warming affects the intensity, frequency, and duration of the rainy season and dry season in tropical climates (Chowdhury et al. 2016).

Global warming is predicted to continue into the next few years. In the projection of future climate change by IPCC-AR5, the earth's temperature will increase along with the increasing concentration of GHG emissions, especially CO_2 gas (IPCC 2014). Projections of future climate change are modeled in a climate change scenario which is called the Representative Concentration Pathway (RCP). The RCP model is divided into four climate change scenarios based on changes in GHG emissions and earth temperature, including: RCP 2.6 (CO_2 concentration = 490 ppm, temperature anomaly = 1.5°); RCP 4.5 (CO_2 concentration = 650 ppm, temperature anomaly = 2.4°); RCP 6.0 (CO_2 concentration = 850 ppm, temperature anomaly = 3.0°); and RCP 8.5 (CO_2 concentration = 1370 ppm, temperature anomaly = 4.9°) (Moss et al. 2010).

As a result of climate change, drought disasters will become increasingly extreme and difficult to detect. In Indonesia, drought has increased in terms of intensity and distribution over time (Surmaini and Faqih 2016). It is consistent with the increasing concentration of CO_2 (by 10 ppm from 2004 to 2010) and air temperatures in Indonesia (Samiaji 2011). Based on data from the National Disaster Management Agency (BNPB), the Sampean Baru watershed located in Bondowoso and Situbondo Regencies is categorized as regions that have very high levels of drought. Drought in this region has had an impact on water management in the Sampean Baru watershed. In recent years, the Regional Disaster Management Agency (BPBD) and the Regional Water Supply Company (PDAM) Bondowoso have collaborated in supplying clean water using water trucks in several areas experiencing drought. Based on clean water dropping data from BPBD and PDAM Bondowoso in 2018, the dropping of clean water has increased both in terms of volume and demand.

Prediction of drought due to the earth's climate change is a necessity to be able to estimate the impact and policies that will be taken in the future. Drought prediction can be

made by utilizing the data of the General Circulation Model (GCM) (Wigena et al. 2015). GCM has been widely used in conducting research related to climate change, including for the assessment of drought (Bayissa et al. 2018; Belayneh et al. 2014; Hwan et al. 2019), assessment of the hydrological cycle (Shamir et al. 2019), predicting reservoir inflow (Halik et al. 2015) and forecast rainfall in an area (Tang et al. 2016). GCM is data that contains parameters of world climate (Mekonnen and Disse 2018). The weakness of GCM is that data is still global and has a coarse-resolution so that it cannot be used directly in simulations (Le et al. 2018). The relationship between global climate and local climate needs to be determined in advance by using empirical functions, so that global climate data can be used at regional/local scale simulations.(Halik and Anwar 2017).

Downscaling techniques have been developed to overcome the problem of the resolution roughness of GCM data. Downscaling techniques are classified into three types, namely: (1) Statistical downscaling, (2) Dynamical downscaling, and (3) Mixed Statistical–Dynamical Downscaling (Wilby and Dawson 2007). Statistical downscaling is a type of downscaling whose processing is cheap and does not require large computational memory (Chen et al. 2011). Besides, spatial and temporal variations in climate variables, especially rainfall, can be effectively explained through statistical downscaling (Sharma et al. 2017). Several statistical downscaling methods have been used in research on climate change, one of which is the Artificial Neural Network (ANN). ANN is very effective in making forecasts that are non-linear when compared to ARIMA (Nayak et al. 2013), SDSM (Campozano et al. 2016), Multiple Linear Regression (MLR) (Riad et al. 2004) and K-Nearest (Eskandarinia et al. 2010). ANN has been used in research on drought prediction (Halik and Anwar 2017).

The Standardized Runoff Index (SRI) is one of the hydrological drought indexes that is needed to determine drought severity (Shukla and Wood 2008). SRI is used to measure the severity of drought based on surface runoff in a watershed and is very suitable in describing the effects of global climate change and land use (Maskey and Trambauer 2015). The drought model based on surface water runoff can complement and improve existing drought indices and future drought levels.

Based on the problems discussed earlier, the purpose of this study is to assess the impact of climate change on drought in the Sampean Baru watershed based on GCM data. This research is expected to be able to contribute to overcoming drought problems in the Sampean Baru watershed and as input for relevant agencies in making policies related to mitigation and adaptation to climate change in the future.

2 Data and method

2.1 Study area

This research was conducted in the Sampean Baru watershed in Bondowoso Regency, East Java. Geographically, the Sampean Baru watershed which has an area of 1260 Km^2, is located between 7° 48′–7° 58′S and 114° 40′–114° 48′E. The watershed's altitude is between 5 and 2444 m above sea level. The watershed is around the Equator so that it directly affects the climate conditions. It is a tropical area which is influenced by monsoon climate. The dry season occurs from June to October and the rainy season occurs from November to May. The average temperature ranged from 27 to 30 °C. The average air humidity ranges from 62 to 69%. The average rainfall in Bondowoso Regency is 5058 mm/

year. Sampean baru reservoir is the main outlet of watershed. This reservoir and the weirs provide irrigation water in the dry season for rice fields with an area of 8613 Ha.
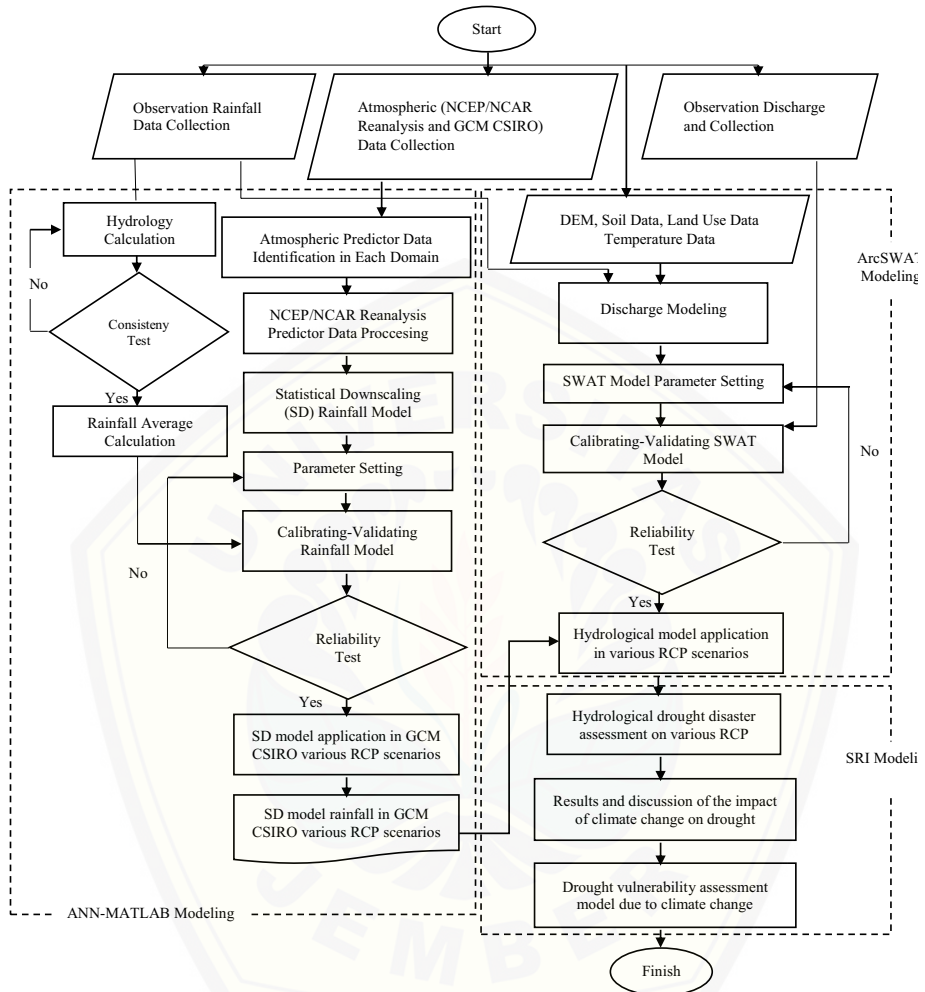
2.2 Data

2.2.1 Observation data

This study uses observational data managed by agencies in Bondowoso Regency. The daily rainfall and discharge data for 30-year period starting from 01/01/1988 to 31/12/2018 managed by the Water Resources Public Works Office of Bondowoso are used to predict rainfall from GCM output. This rainfall data is available at 28 recording stations spread across the study area. The rainfall area is processed and analyzed using aritmethic average method. The observed monthly temperature data was obtained from Meteorology Climatology and

Geophysics Council (BMKG) Banyuwangi. This data is used as an input in any stages of discharge simulation. Digital Elevation Model (DEM) data, soil characteristics, and land use are used to simulate river flow rates. ASTER 30 M DEM data obtained from the United States Geological Survey (USGS) website is used to perform earth surface relief imaging. Land use data were obtained from the Geospatial Information Agency (BIG) of Indonesia. Clean water-dropping data for 2018 obtained from the BPBD are used to control the drought simulation.

2.2.2 Climate projection data

The scenario of future climate change projections has been mathematically modelled. Projections of future climate change are modelled in a climate change scenario which is called the Representative Concentration Pathway (RCP). The RCP model is divided into four climate change scenarios based on changes in GHG emissions and earth temperature, including: RCP 2.6 (CO_2 concentration = 490 ppm, temperature anomaly = 1.5°); RCP 4.5 (CO_2 concentration = 650 ppm, temperature anomaly = 2.4°); RCP 6.0 (CO_2 concentration = 850 ppm, temperature anomaly = 3.0°); and RCP 8.5 (CO_2 concentration = 1370 ppm, temperature anomaly = 4.9°) (Moss et al. 2010). These RCPs contained in GCM data. The General Circulation Model (GCM) is a representation of important processes of the climate system on earth (IPCC 2014). GCM has an output form of grids measuring 100–250 km, according to latitude and longitude (Halik and Anwar 2017). GCM is used to simulate weather, climate understanding, and climate change studies due to changes in CO_2 (Mechoso et al. 2015). According to Smith and Dennis (1989), GCM has advantages with the scenario approach, namely: (1) The model can be used to estimate global climate change in response to an increase in GHG. (2) Estimation of climate variables (such as rainfall, temperature, and humidity) physically according to physical models. (3) Estimates of weather variables (such as wind, radiation, cloud cover, and soil moisture) are sufficient to enter the model. (4) It can simulate the diversity of the daily cycle climate. However, this GCM model also has limitations, including (1) Spatial resolution on a global scale, resulting in gaps between global, regional, and local climate simulation results. (2) This model is difficult to match with ocean circulation models. (3) Atmospheric-biosphere feedback processes are not fulfilled.

In the fifth assessment report, the IPCC has succeeded in overcoming GCM's weaknesses in coupling the ocean circulation model (IPCC 2014). Various developed countries have developed GCM models with different spatial resolutions. This study uses GCM CSIRO Mk 3.6.0 with a resolution of $1.9° \times 1.9°$ developed by Australia because it had been applied to assess meteorological drought in Sampean Baru watershed and gave a good result (Anwar et al. 2014). It also has a coarse spatial resolution. The spatial resolution of GCM data can be overcome using downscaling techniques.

The downscaling model is a method developed to bridge between global/large-scale atmospheric data (temperature, humidity, wind speed, etc.) with local climatic conditions (rainfall) at specific intervals (ARCC 2014). This model is based on the view that global-scale climate influences regional/local-scale climate (Berliana and Sutikno 2007). The problem of low resolution in GCM data can be overcome by using downscaling techniques (Jadmiko and Murdiyarso 2017). Downscaling models are divided into two types, namely: Dynamic Downscaling (DD) Model and Statistical Downscaling (SD) Model (Sharma et al. 2017). DD model is a downscaling process that is carried out on a regional scale grid following changes in the same predictor variables on a global scale grid (GCM) to

simulate a local scale climate (Shamir et al. 2019). The limitation of the DD model is that it requires a long computational time to get results with good resolution (Le et al. 2018). The SD model is a downscaling approach based on empirical relationships between several variables (predictors) on a global/large-scale grid (GCM) and smaller-scale local (predictor) variables (Chen et al. 2011). Predictors used in this study are shown in Table 1. One of the advantages of the SD model compared to the DD model is the fast computing process in assessing the impact of local climate change (Wilby 2002). Therefore, this study uses the SD model.

Artificial Neural Networks (ANN) is the development of an empirical relationship or transfer function of SD between predictor and predictand variables by the non-linear regression method (Halik and Anwar, 2017). ANN is often used in modelling downscaling of precipitation data because of ANN's ability to overcome the non-linear relationship problems of each meteorological–climatological parameter and the nonlinearity of time series data (Retalis et al. 2017; Taiwo et al. 2018; Salimi et al. 2019). ANN gives better downscaling results compared to the SD model linear regression method such as ARIMA (Nayak et al. 2013), SDSM (Campozano et al. 2016), Multiple Linear Regression (MLR) (Riad et al. 2004) and K-Nearest (Eskandarinia et al. 2010) (Fig. 1).

The concept of ANN is designed to resemble the work system of the human brain. It makes ANN have the ability to learn and adapt to new things (Retalis et al. 2017). Like the structure of neurons in the human brain, ANN has artificial neurons, which are simple mathematical models. In the process, the information will be received by the input of the neuron and given weight. Then the artificial neuron body processes the input data through the transfer function. The results of processing are displayed in the neuron output section (Krenker et al. 2011). The ANN approach is performed on MATLAB software. The ANN Architecture is shown in Fig. 2. A simple mathematical model in the process of artificial neurons is expressed in the equation below:

$$y(k) = F\left(\sum_{t=0}^{m} w_i(k) \cdot x_i(k) + b \right) \tag{1}$$

where x_i = input value, w_i = weight value, b = bias, F = transfer function, $y(k)$ = output value.

2.3 Drought indices

Drought is a natural disaster that occurs slowly. It raises obstacles in determining the beginning and end of a drought, the area affected, and the severity (Wilhite 2000). Over time, several drought indexes have been developed to be applied to various types of

Table 1 GCM parameters as predictors in statistical downscaling

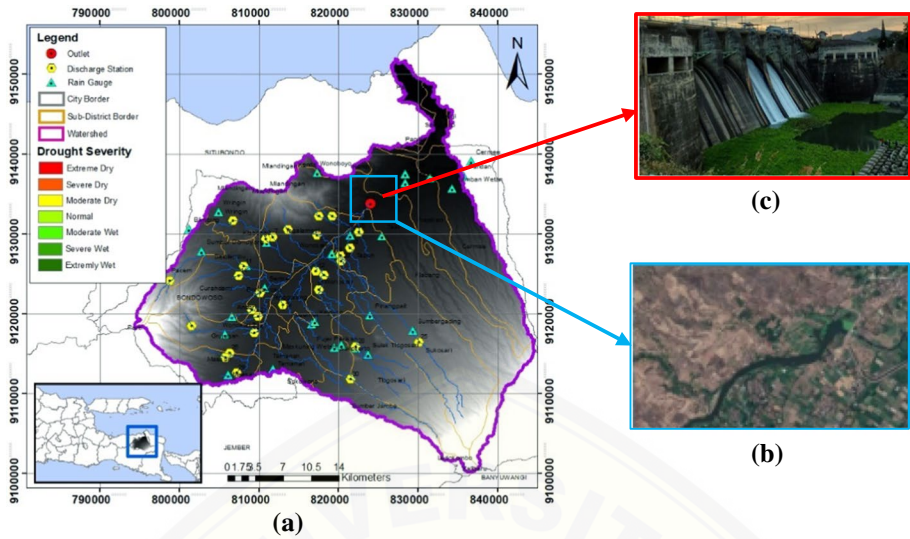| No.	Predictor	Surface	Atmosphere height	
			500 hPa	850 hPa
1	Relative humidity	–	rhum 500	rhum850
2	Specific humidity	–	shum500	rhum850
3	Precipitation water	prec_wtr	–	–
4	Zonal velocity component	uwd	uwd500	uwd850
5	Meridional velocity component	vwd		vwd850

Fig. 1 **a** Sampean Baru watershed map as a research location; **b** the complex geometry of the sampean river; and **c** The Sampean Baru watershed outlet is the Sampean Baru Dam

Fig. 2 ANN Architecture
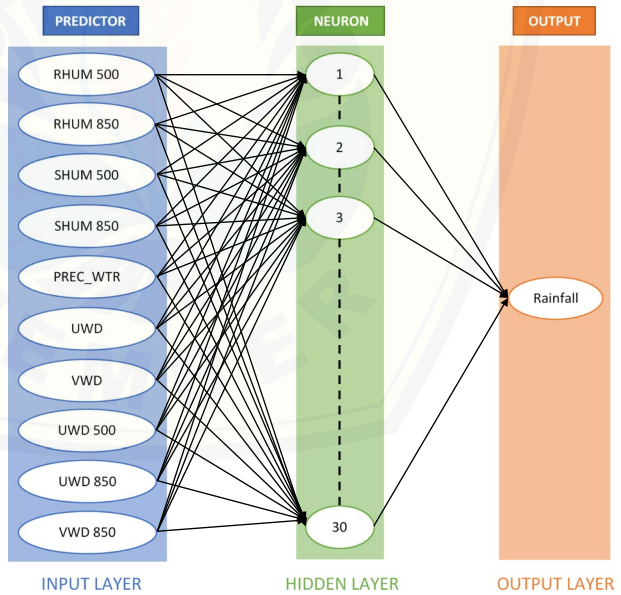
drought (Hwan et al. 2019). One of the drought indices used in this study is the Standardized Runoff Index (SRI). This drought index is used to determine the severity of hydrological drought types. SRI applies the concept of the Standardized Precipitation Index (SPI), where the accumulated surface flow discharge data for a certain period recorded on a discharge station is used as input data. There are some steps to calculate SRI: (1) The time series of runoff is obtained from the simulation. Simulation runoff has the same probability

Table 2 SRI drought categories

SRI value	Drought category
0 to −0.99	Normal
−1 to −1.49	Moderate dry
−1.5 to −1.99	Severe dry
−2 and less	Extreme dry

Table 3 Classification of accuracy result (Adapted from Almeida et al. 2018)

No.	NSE	R^2	Category
1	$0.75 < \text{NSE} \leq 1.00$	$0.75 < \text{NSE} \leq 1.00$	Very good
2	$0.65 < \text{NSE} \leq 0.75$	$0.65 < \text{NSE} \leq 0.75$	Good
3	$0.36 < \text{NSE} \leq 0.65$	$0.50 < \text{NSE} \leq 0.65$	Satisfactory
4	$0.00 < \text{NSE} \leq 0.36$	$0.25 < \text{NSE} \leq 0.50$	Bad
5	$\text{NSE} \leq 0.00$	$\text{NSE} \leq 0.25$	Inappropriate

distribution as observation runoff; (2) Data with the same distribution are used to calculate the cumulative probability of runoff under study; (3) The cumulative probability is converted into a normal distribution using the gamma distribution (Shukla and Wood 2008). The SRI-6 value on each discharge station were mapped using the IDW spatial interpolation method. The SRI and SPI drought categories are similar. It is shown in Table 2. Arc-SWAT 2012.10.3.19 model is used to simulate surface flow discharge. The Soil and Water Assessment Tool (SWAT) is a comprehensive, semi-distributed, continuous-time, process-based model (Abbaspour et al. 2015; Neitsch et al. 2005). Model calibration and validation are needed to determine the accuracy of the model. The calibration process is carried out by determining the value of the model parameters so that the simulation results can approximate the observation data. In this study, manual calibration of SWAT parameter model was applied. The validation process is based on a model with calibrated parameters by entering other data that is not the same as the calibration data, then the simulation results are compared with the observation data (Arnold et al. 2012). The purpose of validation is to prove that the model provides accurate results according to research standards, so that the model can be used to perform simulations with different scenarios (Marek et al. 2016). The accuracy of the model in this study is based on the values of R^2 and NSE (Almeida et al. 2018) is shown in Table 3.

3 Result and discussion

3.1 Statistical downscaling model

The Rainfall-SD model uses ANN assistance. The purpose of this modelling is to get rain predictions for the next 30 years. ANN architecture uses a multilayer perceptron network and backpropagation learning methods. Backpropagation is a supervised learning method based on input and output values. The average observation rainfall data for the Sampean Baru watershed area is used as the target data (predictants), while the atmospheric circulation data for NCEP/NCAR Re-Analysis is used as input data (predictors). In order for

Table 4 Correlation results for Each NCEP/NCAR Grid domain

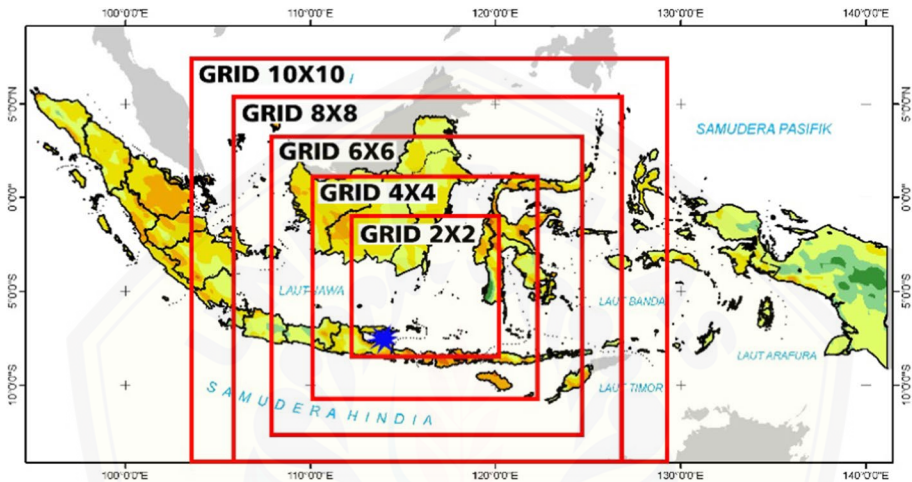| No	Grid domain	Correlation
1	2×2	5.99
2	4×4	6.09
3	6×6	5.07
4	8×8	4.98
5	10×10	4.29

Fig. 3 Research sites and NCEP/NCAR gid domains

NCEP/NCAR Re-Analysis data to be processed in a downscaling model, the local scale needs to be processed and represented in the form of a grid domain. In determining the optimal grid domain there are no special provisions. Correlation results on various NCEP/NCAR atmospheric circulation data grid domains can be seen in Table 4 and Fig. 3. The result of the highest correlation calculation shows that the optimal NCEP/NCAR grid domain that can be used in the ANN process is a 4×4 grid domain with a correlation value of 6.09. Determination of the CSIRO Mk 3.6.0 grid domain is done by adjusting the coordinate position to the NCEP/NCAR 4×4 grid domain. The adjustment results show that the CSIRO Mk 3.6.0 grid domain used is a 6×6 grid domain which can be seen at Fig. 4.

Predictor data contained in the optimal NCEP/NCAR grid is used in the ANN process. The ANN training phase was carried out in the monthly rainy period of 1988–2009, while the model validation phase was 2010–2014 and the testing phase was 2015–2018. This division of training and validation periods is a technique to achieve an optimal solution to overfitting. While the testing period is only to test the ability of the resulting ANN. The activation functions considered include: linear functions (purelin), non-linear functions (log-sigmoid and tan-sigmoid). The selection of the activation function from the input layer to the hidden layer and to the output layer as well as the optimal number of units in the hidden layer is based on the lowest MSE (Mean Square Error) value. An update of the weights using the Levenberg-Marquadt method. The results of ANN running show that the optimal ANN architecture is achieved with thirty hidden layer neurons with activation functions of
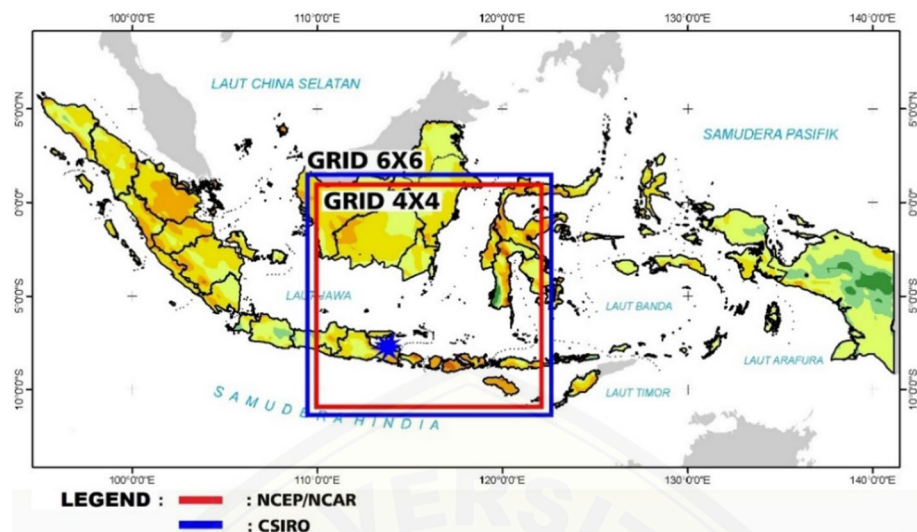
Fig. 4 CSIRO Mk 3.6.0 grid domains

tansig in the hidden layer and purelin in the output layer. The coefficient determination in each phase close to 1 that can be seen in Table 5. It means that the artificial rainfall using NCEP/NCAR Re-Analysis data during 1988–2018 is approximate to observation rainfall data.

The ANN model of rainfall due to climate change uses CSIRO Mk 3.6.0 atmospheric circulation data. This GCM data has three climate change scenarios based on an increase in greenhouse gas emissions or CO2 gas in the atmosphere by 1% per year, namely RCP 4.5, RCP 6.0, and RCP 8.5. The RCPs data are used as predictors. ANN training was carried out on monthly rainfall for the 2006–2016 period, while the validation period was 2017 and the testing period was 2018. The activation functions considered include: linear functions (purelin), non-linear functions (log-sigmoid and tan-sigmoid). The selection of the activation function from the input layer to the hidden layer and to the output layer as well as the optimal number of units in the hidden layer is based on the lowest MSE (Mean Square Error) value. The optimal ANN architecture is achieved with 30 hidden layer neurons with activation functions of tansig in the hidden layer and purelin in the output layer. An update of the weights using the Levenberg-Marquadt method. The results of the ANN process on each GCM can be seen in Table 5. In general, the ANN model gives good results. It can

Table 5 ANN model reliability test on NCEP/NCAR Reanalysis and CSIRO Mk.3.6.0 scenarios

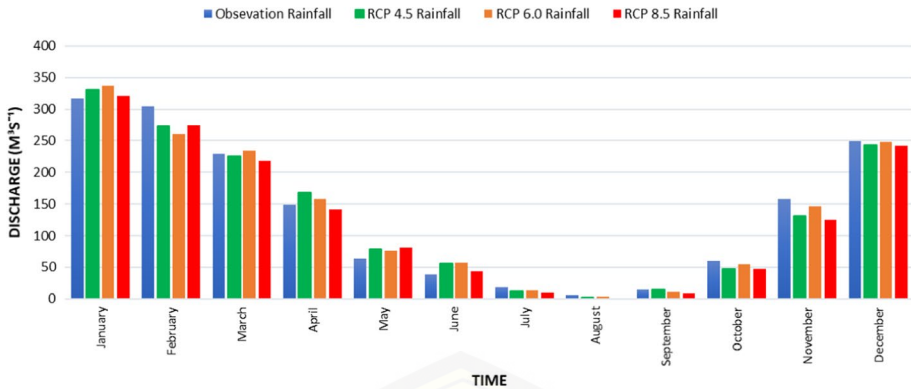| Phase | NCEP/NCAR Re-analysis | | CSIRO Mk 3.6.0 | | | | | |
| | | | RCP 4.5 | | RCP 6.0 | | RCP 8.5 | |
	R	RMSE	*R*	RMSE	*R*	RMSE	*R*	RMSE
Training	0.89	61.27	0.88	61.71	0.87	61.40	0.89	60.91
Validation	0.91	53.04	0.93	70.60	0.96	52.89	0.96	38.51
Testing	0.94	55.01	0.98	28.63	0.81	67.21	0.88	57.83

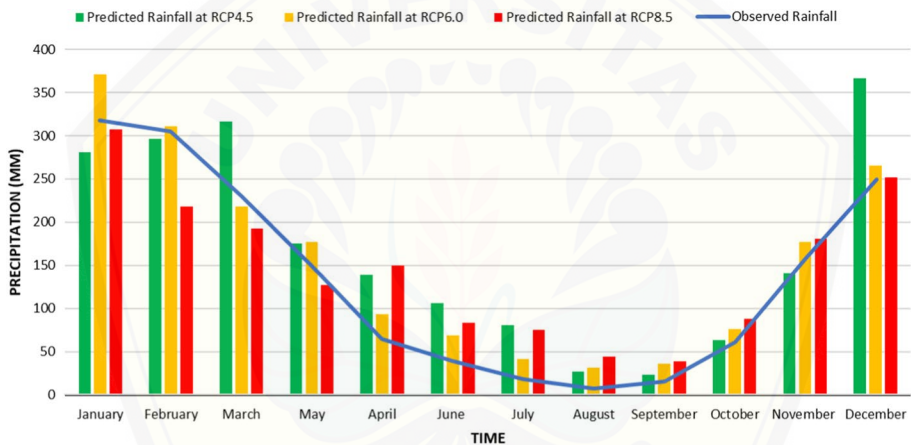**Fig. 5** Graphic plot of observation and CSIRO Mk 3.6.0 rainfall in 2006–2018

Fig. 6 Predicted monthly rainfall based on CSIRO Mk 3.6.0 data: **a** RCP4.5 Scenario; **b** RCP6.0 Scenario; **c** RCP8.5 Scenario

be seen from the coefficient of determination in each of RCPs producing values that are close to 1. The average monthly rainfall plot ANN model gives results that are close to the monthly average rainfall plots of observation can be seen in Fig. 5.

The results of downscaling process for GCM data in 2006–2018 are the basis or reference for predicting rainfall until 2050. The GCM data in 2019–2050 is used as an input in ANN process. The results show that ANN can model rainfall predictions using GCM data. Comparison between monthly rainfall prediction results for the next 30 years (2019–2050) uses GCM data and monthly observed rainfall data can be seen in Fig. 6. The predicted monthly rainfall of RCP 6.0 has a trend-line that resembles the observed monthly rainfall compared to the other RCPs. The predicted monthly rainfall of RCP 6.0 has a slightly higher intensity than the observed monthly rainfall except for March. In RCP 6.0, the highest and lowest predicted monthly rainfall will occur in January and August. The predicted monthly rainfall of RCP 4.5 has a different trend from the observed monthly rainfall. Predictions of the highest and lowest rainfall occur in December and September. The predicted

monthly rainfall of RCP 8.5 also has a different trend-line from the observed monthly rainfall. The increase in rainfall intensity occurred in April where the trend line experienced a slope from January to March. Predictions of the highest and lowest rainfall occur in January and September.

3.2 Drought indices model

In the SRI drought model, hydrological modelling is an important component to get the temporal river discharge at each observation station. SWAT modelling divides the Sampean Baru watershed into 21 sub-watersheds with river outlets in the Sampean Baru Dam. In the first stage, discharge simulation is carried out using observation rainfall data and observed temperature data as an input. The results of the simulation before calibration show that discharge simulation is still not close to the observation discharge. This can be seen from the low NSE value which can be categorized as bad, even though R^2 value has good results. The calibration process needs to be carried out through a process of selecting a combination of parameters so that the coherence between the observed discharge and the simulated discharge increases. The calibration process was carried out on simulated discharge data from 1988 to 2007. Some of the parameters selected in the calibration process can be seen in Table 6. Discharge simulation after calibration shows good results that can be seen as an increase in the value of R^2 and NSE. This also shows that the selected parameter values are able to represent the actual conditions in the field and are suitable for use in the validation process. The validation process was carried out on simulated discharge data from 2008 to 2018. The validation process shows satisfactory results where the value of R squared and NSE is above 0.7. It also shows that the model provides consistent results according to the established standards. The result of calibration and validation process are presented in Table 7 and Fig. 7.

The validated model is used to predict the discharge simulation. The predictive discharge simulation uses NCEP/NCAR Reanalysis artificial and GCM rainfall data as input data. Discharge simulation using artificial rainfall NCEP/NCAR Reanalysis in 1988–2018 gave R Square and NSE results with very good categories. The same results were also shown in the discharge simulation using GCM artificial rainfall in 2006–2018. The discharge simulation on each RCP gives R Square and NSE results with very good category. It is shown in Fig. 8 that the model responds well to artificial rainfall so that it possible to perform discharge prediction. The reliability test results are presented in Table 8. Comparison between predicted monthly discharge results for the next 30 years (2019–2050) uses GCM data and monthly observed discharge data can be seen in Fig. 9. The predicted monthly discharge of RCP 6.0 has a trend-line that resembles the observed monthly discharge compared to the other RCPs. The predicted

Table 6 The reliability test of discharge simulation

Model performances	Input data		
	Observation rainfall		
	Before calibrating	After calibrating	Validating
Coefficient of performance (R^2)	0.7051	0.7528	0.7993
Nash–Sutcliffe Efficiency (NSE)	0.2437	0.7422	0.7782

Table 7 Parameters used from SWAT Model and its calibrated value

| No	Parameters	Meaning	Initial value	Fitted value
1	CN2	Moistures condition II number curve	35–98	81.2
2	ALPHA_BF	Baseflow reccession constant	0.048	0.048
3	GWDELAY	Delay time for aquifer recharge (days)	31	155.3
4	GWQMN	Threshold water level in shallow aquifer for baseflow (mmH2O)	1000	3366.7
5	RCHRG_DP	Aquifer percolation coefficient	0.05	0.045
6	SOL_K	Saturated hydraulic conductivity of first layer (mm/hr)	4.93	9.367
7	SOL_AWC	Available water capacity	0.178	0.1246
8	ESCO	Soil evaporation compensation coefficient	0.95	0.665
9	HRU_SLP	Average slope steepness (m/m)	0.046	0.0644
10	SLSSUBBSN	Average slope length (m)	91.463	100.6093
11	CH_K2	Effective hydraulic conductivity of channel (mm/hr)	0	0
12	CH_N2	Manning's "n" value for the main channel	0.014	0.0014
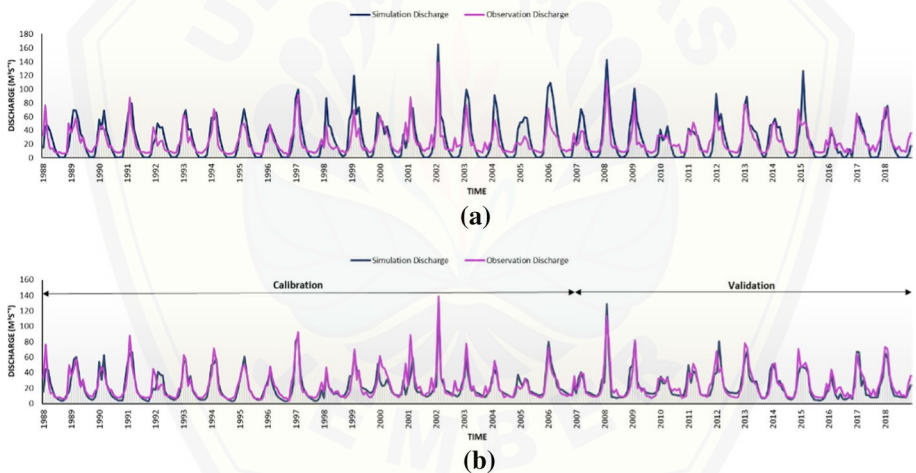
Fig. 7 Discharge simulation using observation rainfall as an input **a** before calibration; **b** after calibration and validation
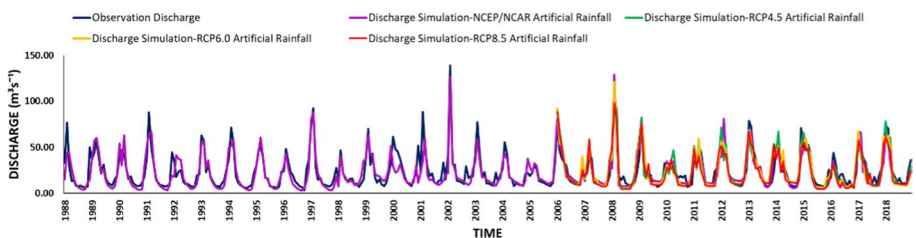

Fig. 8 Discharge simulation using NCEP/NCAR Reanalysis and CSIRO Mk 3.6.0 rainfall as an input

Table 8 The reliability test of discharge simulation

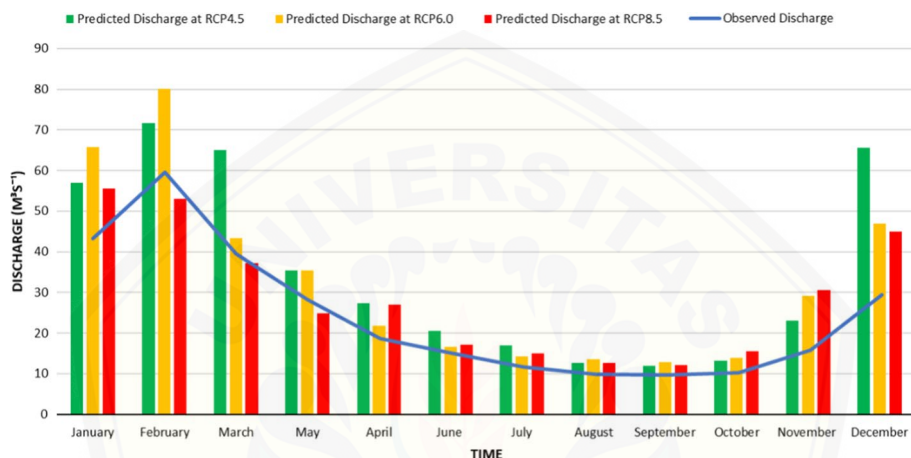| Model performances	Input data			
	NCEP/NCAR reanalysis rainfall	RCP 4.5	RCP 6.0	RCP 8.5
Coefficient of performance (R^2)	0.7817	0.8074	0.8019	0.8068
Nash–Sutcliffe Efficiency (NSE)	0.7521	0.7806	0.7802	0.7872

Fig. 9 Predicted monthly discharge based on CSIRO Mk 3.6.0 rainfall data **a** RCP 4.5 Scenario; **b** RCP 6.0 Scenario; **c** RCP 8.5 Scenario

monthly discharge of RCP 6.0 has a slightly higher intensity than the observed monthly discharge. In RCP 6.0, the highest and lowest predicted monthly discharge will occur in February and September. The predicted monthly discharge of RCP 4.5 has a different trend from the observed monthly discharge. Predictions of the highest and lowest discharge occur in February and September. The predicted monthly discharge of RCP 8.5 also has a different trend-line from the observed monthly discharge. The increase in discharge intensity occurred in April where the trend line experienced a slope from January to March. Predictions of the highest and lowest discharge occur in January and September.

Analysis of the severity of SRI dryness uses a time scale of discharge deficits for six months (SRI-6). Based on Fig. 10, the hydrological drought in Bondowoso Regency with an extremely dry category ($SRI < -2$) occurred in 1996, 1998, and 2016. The results of the drought index were compared with data on water distribution to drought-affected areas in 2018 which was obtained from BPBD Bondowoso, so that, it can be seen suitability to the actual conditions. Based on BPBD data on the water distribution data in 2018, several areas in Bondowoso Regency experienced drought, including wringin, jatisari, pameton, karangsengon, botolinggo, and gayam villages. It is consistent with the results of the Fig. 11 drought model, wherein the villages of Wringin, Jatisari, Pameton, Karangsengon, Botolinggo, and Gayam also experienced drought in
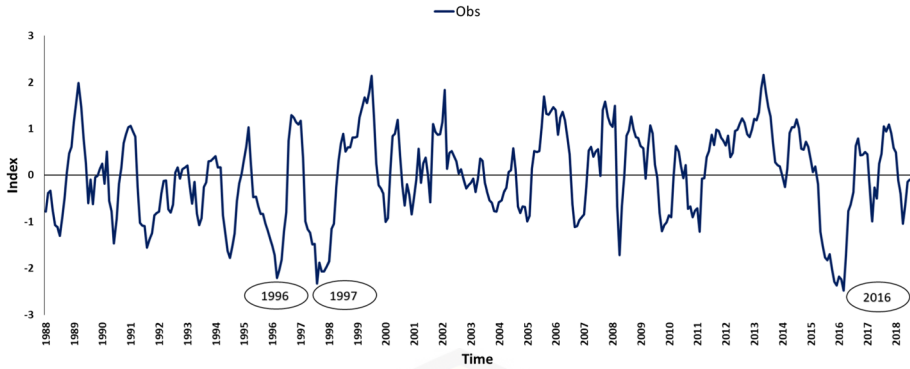
Fig. 10 Plotting of SRI-6 drought index in the Sampean Baru watershed
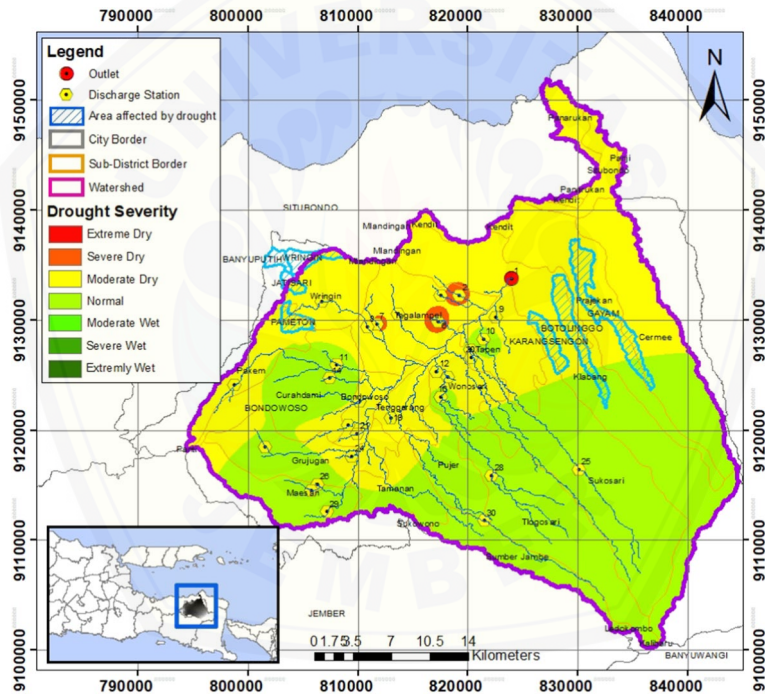

Fig. 11 Spatial map of SRI-6 drought severity in 2018

the moderate dry category ($-1 < \text{SRI} < -1.5$). Based on the analysis results, the SRI-6 drought model can represent the drought that occurred in Bondowoso Regency.

The prediction of the SRI drought in Sampean Baru watershed is based on the climate change scenario contained in the GCM CSIRO Mk 3.6.0 data. Predictive discharge data on various RCPs obtained from rainfall-flow simulation are then used as input data on the drought model. The results of drought predictions on various RCPs are shown in Fig. 12. The RCP 4.5 is a scenario that does not have extreme drought severity. The
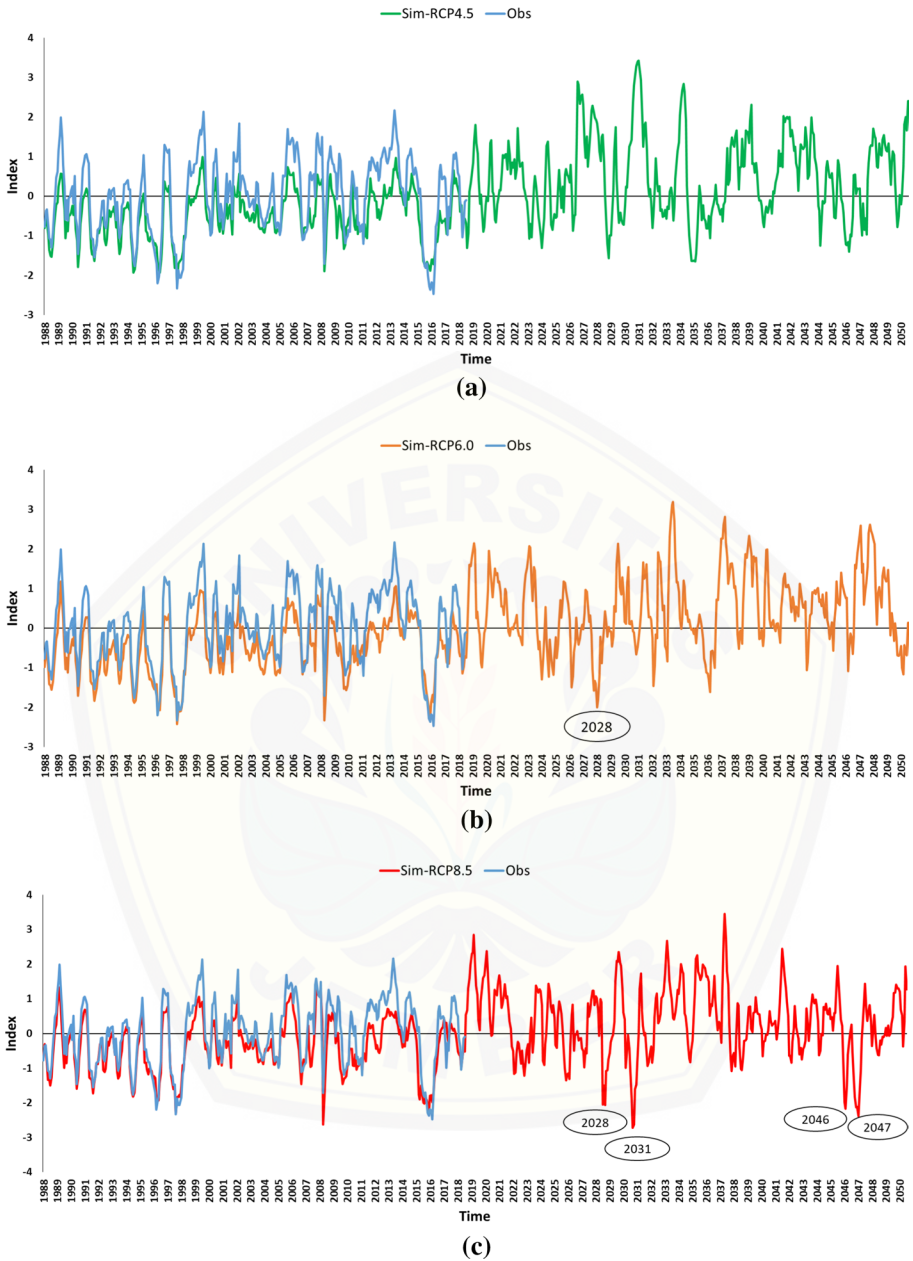
Fig. 12 The SRI drought prediction based on CSIRO Mk 3.6.0 data **a** RCP4.5; **b** RCP6.0; **c** RCP8.5

average drought index of RCP 4.5 is 0.48 which categorizes as a normal. The RCP 6.0 and RCP 8.5 have extreme drought levels. Extreme drought in RCP 6.0 will occur in 2028. At RCP 8.5, extreme drought will occur in 2028, 2031, 2046, and 2047. The average drought index of The RCP 6.0 and RCP 8.5 are 0.49 and 0.36. Both of them are

Table 9 Number of drought event in each category

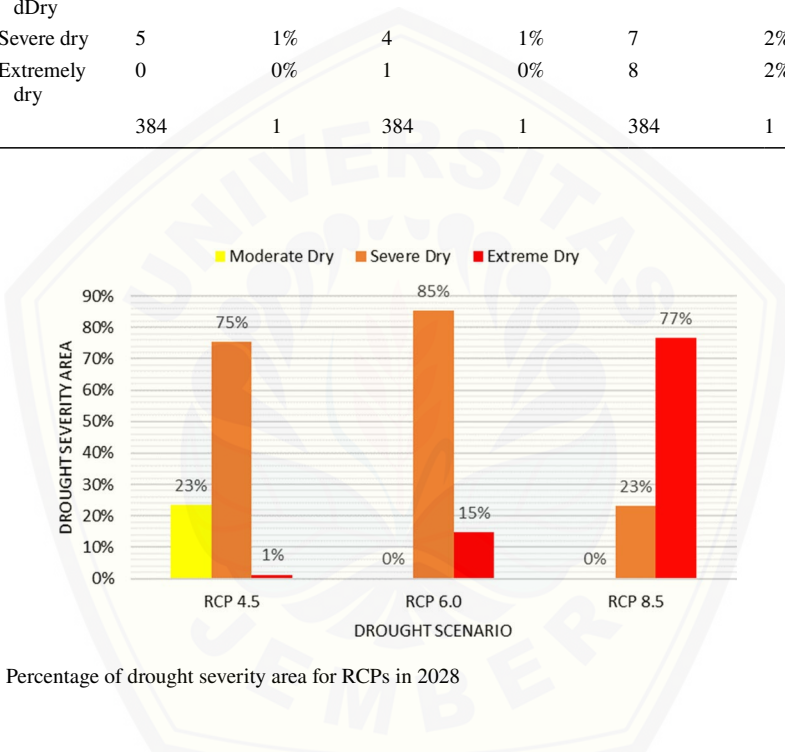| No.	Category	RCP 4.5		RCP 6.0		RCP 8.5	
		Drought event	Percentage	Drought event	Percentage	Drought event	Percentage
1	Extremely wet	28	7%	26	7%	17	4%
2	Severe wet	35	9%	37	10%	33	9%
3	Moderate wet	57	15%	52	14%	55	14%
4	Normal	240	63%	246	64%	248	65%
6	Moderate dDry	19	5%	18	5%	16	4%
7	Severe dry	5	1%	4	1%	7	2%
8	Extremely dry	0	0%	1	0%	8	2%
Total		384	1	384	1	384	1

Fig. 13 Percentage of drought severity area for RCPs in 2028

categorized as a normal. In Table 9, it shows number of drought event in each category. There is no extreme dry event at RCP 4.5. The RCP 6.0 has one extreme dry event. There are eight extreme drought events at RCP 8.5.

The effect of the increase in the GHG concentration found in each RCP scenario can be seen in the graph of the drought severity distribution in 2028 in Fig. 13. The area affected by extreme drought has increased by 15 and 77% in RCP6.0 and RCP8.5. It is in line with the increasing number of districts affected by extreme drought, which can be seen in Fig. 14. On the RCP 4.5 output drought distribution map in 2028, extreme drought conditions occurred in 2 districts, namely Tegalampel and Klabang. On the RCP 6.0 output drought distribution map in 2028, extreme drought conditions occurred in 9 districts, namely Wringin, Tegalampel, Klabang, Sukosari, Tlogosari, Sumberjambe, Pujer, Maesan, and Grujugan. On the map of RCP 8.5 drought distribution in 2028, extreme drought conditions occurred in 15 sub-districts, namely Pakem, Curahdami,
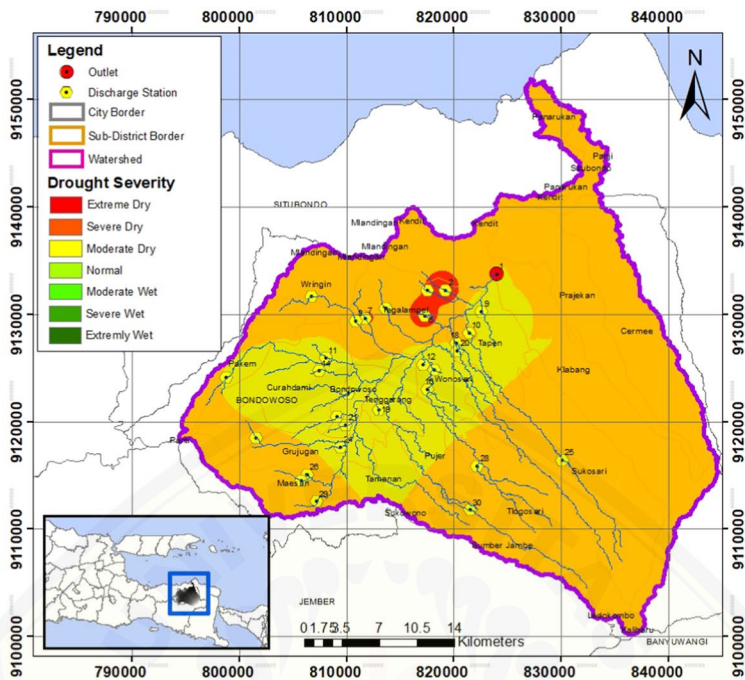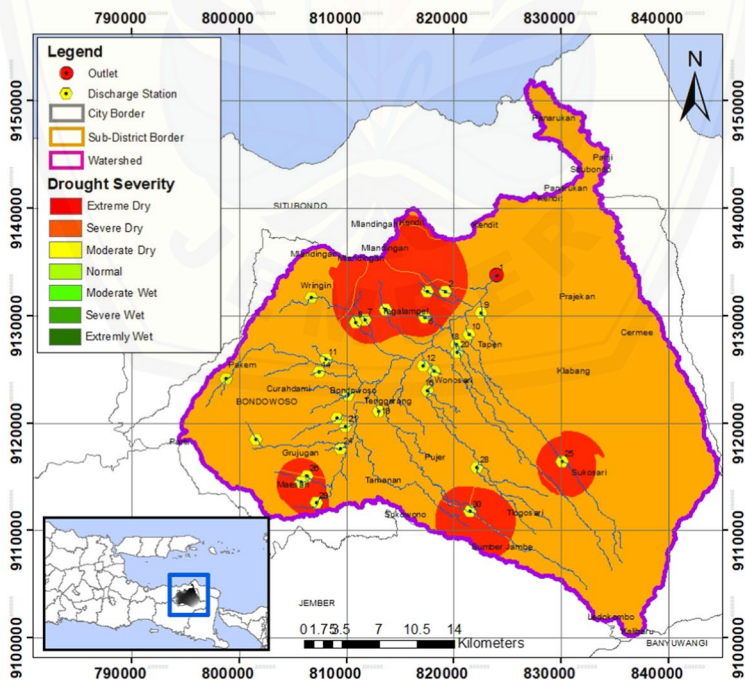
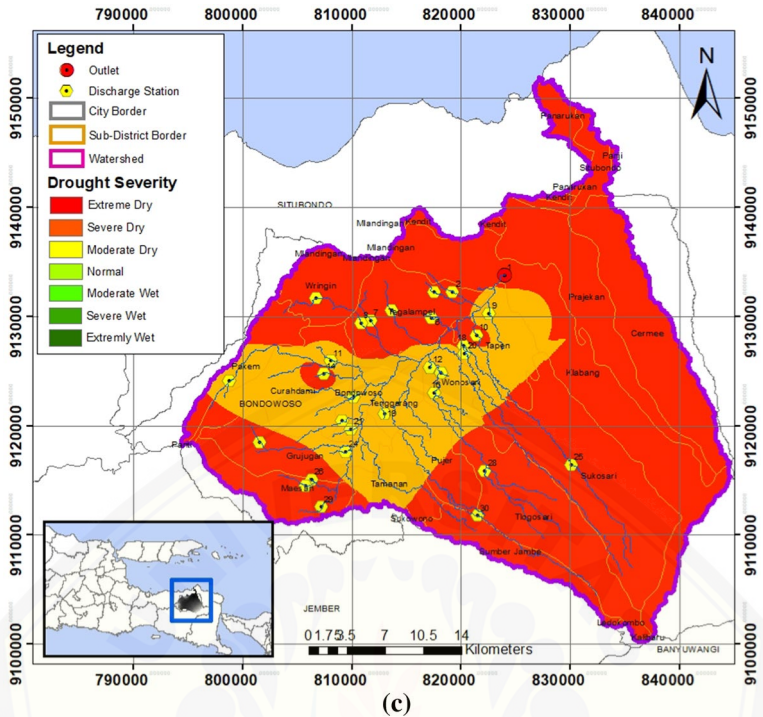**Fig. 14** Spatial drought map in 2028 **a** RCP4.5; **b** RCP6.0; **c** RCP8.5

Fig. 14 (continued)

Wringin, Tegalampel, Klabang, Prajekan, Cerme, Tapen, Sukosari, Tlogosari, Sumberjambe, Pujer, Tamanan, Maesan, and Grujugan.

4 Conclusions

The statistical downscaling (ANN) to simulate monthly rainfall using NCEP/NCAR and CSIRO Mk 3.6.0 shows a good result. It can be seen that the simulated monthly rainfall value resembles the observed monthly rainfall value. The ANN also simulate the predicted monthly rainfall in each RCPs. The result of downscaling shows that the trend of predicted monthly rainfall at RCP 6.0 is closer to monthly observed rainfall than the other RCPs. It gives impact on the result of predicted discharge that shows the trend of RCP 6.0 is closer to monthly observed discharge than the other RCPs. Assessing impact of climate change on drought using GCM successfully represented the predicted drought conditions in the Sampean Baru Watershed. A 6-month time scale of SRI (SRI-6) was chosen to assess drought. It is based on good correlation between drought severity map in 2018 and clean water distribution data in 2018. Increased greenhouse gas concentrations (GHG) influence the intensity of drought events and drought-affected areas in future. The number of extreme drought events has increased in each RCP. RCP 8.5 has the highest number of extreme drought events, followed by RCP 6.0. RCP 4.5 has no extreme drought events. The area of extreme drought has also increased quite significantly.

Declarations

Conflict of interest The authors have no conflicts of interest to declare that are relevant to the content of this article.

References

Abbaspour KC, Rouholahnejad E, Vaghefi S, Srinivasan R, Yang H, Kløve B (2015) A continental-scale hydrology and water quality model for europe: calibration and uncertainty of a high-resolution large-scale SWAT Model. J Hydrol 524:733–752. https://doi.org/10.1016/j.jhydrol.2015.03.027

Almeida RA, Pereira SB, Pinto DBF (2018) Calibration and validation of the SWAT hydrological model for the Mucuri River Basin SWAT-CUP. Journal of the Brazzilian Association of Agricultural Engineering 4430:55–63

Anderson TR, Hawkins E, Jones PD (2016) CO2, The greenhouse effect and global warming: from the pioneering work of arrhenius and callendar to today's earth system models. Endeavour 40(3):178–187. https://doi.org/10.1016/j.endeavour.2016.07.002

Anwar N, Halik G, Edijanto (2014) Statistical downscaling model for assessing drought disaster due to climate change at Sampean Watershed, Indonesia. International Congress on Irrigation and Drainage 17(September):66

ARCC (2014) A review of downscaling methods for climate change projections. US Agency International Development.

Arnold JG, Moriasi D, Gassman P, Abbaspour K, White M, Srinivasan R, Santhi C, Harmel RD, Van Griensven A, Van Liew MW, Kannan N (2012) SWAT: model use, calibration, and validation. Trans ASABE 55(4):1491–1508

Bayissa Y, Blue U, Basin N, Maskey S, Id TT, Van Andel SJ (2018) Comparison of the performance of six drought indices in characterizing historical drought for The Upper Blue Nile Basin. Ethiopia. Geosciences 8(81):1–26. https://doi.org/10.3390/geosciences8030081

Belayneh A, Adamowski J, Khalil B, Ozga-zielinski B (2014) Long-term SPI drought forecasting in the Awash River Basin in Ethiopia using wavelet neural network and wavelet support vector regression models. J Hydrol 508:418–429. https://doi.org/10.1016/j.jhydrol.2013.10.052

Berliana S, Sutikno S (2007) Kajian Dampak Pemanasan Global Terhadap Pola Curah Hujan Indonesia dengan Menggunakan Statistik Downscaling. Statistika 7(2):5–12

Campozano L, Tenelanda D, Sanchez E, Samaniego E, Feyen J (2016) Comparison of statistical downscaling methods for monthly total precipitation: case study for the Paute River Basin in Southern Ecuador. Adv Meteraol. https://doi.org/10.1155/2016/6526341

Chen J, Brissette FP, Leconte R (2011) Uncertainty of downscaling method in quantifying the impact of climate change on hydrology. J Hydrol 401(3–4):190–202. https://doi.org/10.1016/j.jhydrol.2011.02.020

Chowdhury R, Mohamed MMA, Murad A (2016) Variability of extreme hydro-climate parameters in the North-Eastern Region of United Arab Emirates. Proc Eng 154:639–644. https://doi.org/10.1016/j.proeng.2016.07.563

Eskandarinia A, Nazarpour H, Teimouri M, Ahmadi M (2010) Comparison of neural network and K-nearest neighbor methods in daily flow forecasting. J Appl Sci 10(11):1006–1010. https://doi.org/10.3923/jas.2010.1006.1010

Halik G, Anwar N (2017) Prediksi Kekeringan Berbasis Data Luaran GCM. ITS Press, Surabaya

Halik G, Anwar N, Santosa B (2015) Reservoir inflow prediction under GCM scenario downscaled by wavelet transform and support vector machine hybrid models. Adv Civil Eng. https://doi.org/10.1155/2015/515376

Hwan M, Eun L, Im S, Bae DH (2019) A comparative assessment of climate change impacts on drought over Korea based on multiple climate projections and multiple drought indices. Clim Dyn. https://doi.org/10.1007/s00382-018-4588-2

IPCC. (2014). Climate Change 2014: Synthesis report. Contribution of Working Groups I, II and III to the Fifth Assessment Report of the Intergovernmental Panel on Climate Change [Core Writing Team,

R.K. Pachauri and L.A. Meyer (eds.)]. In *IPCC, Geneva, Switzerland, 151pp*. https://doi.org/10.1046/j.1365-2559.2002.1340a.x

Jadmiko SD, Murdiyarso D (2017) Koreksi Bias Luaran Model Iklim Regional untuk Analisis Kekeringan Bias correction of Regional Climate Model Outputs for Drought Analysis. Jurnal Tanah Dan Iklim 41:25–36

Krenker A, Bešter J, Kos A (2011) Introduction to the Artificial Neural Networks. In: Suzuki (ed) Artificial neural network-methodological advances and biomedical applications. Rijeka: InTech.

Kweku DW, Bismark O, Maxwell A (2018) Greenhouse effect: greenhouse gases and their impact on global warming greenhouse effect: greenhouse gases and their impact on global warming. J Sci Res Reports 17(6):1–9. https://doi.org/10.9734/JSRR/2017/39630

Le R, Katurji M, Zawar-reza P (2018) Comparison of statistical and dynamical downscaling results from the WRF model. Environ Model Software J 100:67–73. https://doi.org/10.1016/j.envsoft.2017.11.002

Marek GW, Gowda PH, Evett SR, Baumhardt RL, Brauer DK, Howell TA, Marek TA, Point I (2016) Calibration and validation of the SWAT model for predicting daily ET over irrigated crops in the texas high plains using lysimetric data. ASABE 59(2):611–622. https://doi.org/10.13031/trans.59.10926

Maskey S, Trambauer P (2015) Hydrological modeling for drought assessment. In: Hazards H-M (ed) Risks, and Disasters. Elsevier, Amsterdam, pp 263–280

Mechoso, C. R., Arakawa, A., & Angeles, L. (2015). General circulation models. In *Encyclopedia of atmospheric sciences 2nd Edition* 2nd edn, Vol. 4. https://doi.org/10.1016/B978-0-12-382225-3.00157-2

Mekonnen DF, Disse M (2018) Analyzing the future climate change of Upper Blue Nile River basin using statistical downscaling techniques. Hydrol Earth Syst Sci 22:2391–2408. https://doi.org/10.5194/hess-22-2391-2018

Moss RH, Edmonds JA, Hibbard KA, Manning MR, Rose SK, Van Vuuren DP, Carter TR, Emori S, Kainuma M, Kram M, Meehl GA, Mitchell JFB, Nakicenovic N, Riahi K, Smith SJ, Stouffer RJ, Thomson AM, Weyant JP, Wilbanks TJ (2010) The next generation of scenarios for climate change research and assessment. Nature 463:747–756. https://doi.org/10.1038/nature08823

Nayak DR, Mahapatra A, Mishra P (2013) A survey on rainfall prediction using Artificial Neural Network. Int J Comp Appl 62(16):32–40. https://doi.org/10.5120/12580-9217

Neitsch SL, Arnold JG, Kiniry JR, Williams J (2005) Soil and water assessment tools theoretical documentation version 2005. Temple, Texas.

Retalis A, Tymvios F, Katsanos D, Michaelides S (2017) Downscaling CHIRPS precipitation data: an artificial neural network modelling approach network modelling approach. Int J Remote Sens 38(13):3943–3959. https://doi.org/10.1080/01431161.2017.1312031

Riad S, Mania J, Polytechnique E, Lille UD, Langevin AP, Najjar Y (2004) Rainfall-runoff model using an Artificial Neural Network Approach. Math Comp Model 40:839–846. https://doi.org/10.1016/j.mcm.2004.10.012

Salimi AH, Samakosh JM, Sharifi E, Hassanvand RM, Noori A, von Rautenkranz H (2019) Optimized Artificial Neural Networks-based methods for statistical downscaling of gridded. MDPI Water. https://doi.org/10.3390/w11081653

Samiaji T (2011) GAS CO2 DI WILAYAH INDONESIA. J Lapan 12(2):68–75. Retrieved from http://jurnal.lapan.go.id/index.php/berita_dirgantara/article/download/1652/1490

Shamir E, Halper E, Modrick T, Georgakakos KP, Chang H, Lahmers TM, Castro C (2019) Statistical and dynamical downscaling impact on projected hydrologic assessment in arid environment: a case study from Bill Williams River basin and Alamo Lake, Arizona. Journal of Hydrology X 10(2):13. https://doi.org/10.1016/j.hydroa.2019.100019

Sharma T, Vittal H, Chhabra S, Salvi K (2017) Understanding the cascade of GCM and downscaling uncertainties in hydro-climatic projections over India. Int J Climatol. https://doi.org/10.1002/joc.5361

Shukla S, Wood AW (2008) Use of a standardized runoff index for characterizing hydrologic drought. Geophys Res Lett 35:1–7. https://doi.org/10.1029/2007GL032487

Sudarma IM, As-syakur AR (2018) Dampak Perubahan Iklim Terhadap Sektor Pertanian di Provinsi Bali. J Socio-Econ Agric Agribus 12(1):87–97. https://doi.org/10.24843/SOCA.2018.v12.i01.p07

Surmaini E, Faqih A (2016) Kejadian Iklim Ekstrem dan Dampaknya Terhadap Pertanian Tanaman Pangan di Indonesia. Jurnal Sumberdaya Lahan 10(2):115–128

Taiwo AI, Folorunso SO, Ogunwobi ZO (2018) Forecast performance of univariate time series and artificial neural network model. J Eng Technol 12(2):67–71

Tang J, Niu X, Wang S, Gao H, Wang X, Wu J (2016) Statistical downscaling and dynamical downscaling of regional climate in China: present climate evaluations and future climate projections. J Geophys Res Atmoss 121:2110–2129. https://doi.org/10.1002/2015JD023977.Received

Wigena AH, Djuraidah A, Sahriman S (2015) Statistical downscaling dengan Pergeseran Waktu Berdasarkan Korelasi Silang. Jurnal Meteorologi Dan Geofisika 16(1):19–24

Wilby RL (2002) sdsm—a decision support tool for the assessment of regional climate change impacts. Environ Model Softw J 17:147–159

Wilby RL, Dawson CW (2007) SDSM 4.2—A decision support tool for the assessment of regional climate change impacts User Manual.

Wilhite DA (2000) Chapter 1 drought as a natural hazard : concepts and definitions. Drought Mitigation Center Faculty Publication, Nebraska

Publisher's Note Springer Nature remains neutral with regard to jurisdictional claims in published maps and institutional affiliations.